A Glimpse of the Large-Scale Equatorial Dynamics: The Equatorial β-Plane Approximation

Tiago Carrilho Biló

C# 11950866

tcb46@miami.edu

Rosenstiel School of Marine and Atmospheric Science - Geophysical Fluid Dynamics I (MPO 611) - Project Report

December 2, 2015

1 Introduction

The present report is part of the Geophysical Fluid Dynamics (GFD) I coursework project. Here I present some aspects of the so-called equatorial β-plane approximation and solutions of the equations of motion under such assumption in the ocean. The solutions presented in the following paragraphs describe oceanic phenomena that are essential to understand the equatorial large-scale dynamics in the Pacific and Atlantic oceans.

Equatorial regions present phenomena related to mass and energy transfer between hemispheres and basins (e.g., North Brazil Current rings, Indonesian throughflow), important to biological production and dynamics (e.g., equatorial upwelling), and result of particular response to local and remote forcing (e.g., El Niño Southern Oscillation). Therefore, low-latitudes circulation is extremely complex and relevant for the understanding of the ocean large-scale circulation, climate variability, and human activities (e.g., *Talley et al.*, 2011).

In order to verify such importance and how useful is the equatorial β-plane approximation, in Section 2 I present what is the equatorial β-plane approximation, key characteristics, some solutions (i.e. stationary and free waves solutions), and how it is applied in the studying of real flows.

2 The equatorial β-plane approximation: characteristics and a few solutions

Geophysical fluid motions are governed by the Newton's second law, also known as the Navier-Stokes equations. In the vectorial form the Navier-Stokes equation can be written as

$$\rho(\frac{D\vec{v}}{Dt} + 2\vec{\Omega} \times \vec{v}) = -\nabla p - \vec{g} + \nabla \cdot (\mu \nabla \vec{v}), \tag{1}$$

(*Pedlosky*, 1987)

where ρ, $\vec{v}$, $\vec{\Omega}$, p, $\vec{g}$, and μ are the fluid's density, three-dimensional velocity vector, Earth's rotation vector, pressure, gravity, and molecular diffusion coefficient respectively. We know that Earth can be thought as a spherical rotating reference frame, therefore the natural representation of Equation 1 is its expansion in the spherical coordinates system. However the study of fluids motion in such system can be exhausting due to its complexity, so it is convenient to work in a rectangle coordinate system (i.e. Cartesian coordinates).

The Cartesian representation of Equation 1 applicable for oceanic motions under the Boussinesq approximation (i.e. ocean $\approx$ incompressible) is given by

$$\begin{cases} \frac{D\vec{v}}{Dt} + f\vec{k} \times \vec{v} = -\frac{\nabla p}{\rho_0} - g'\vec{k} + \nabla \cdot (\frac{\mu}{\rho_0} \nabla \vec{v}); \\ \vec{v} = u\vec{i} + v\vec{j} + w\vec{k}; \\ \frac{D}{Dt} = \frac{\partial}{\partial t} + u\frac{\partial}{\partial x} + v\frac{\partial}{\partial y} + w\frac{\partial}{\partial z}; \\ \nabla = \frac{\partial}{\partial x}\vec{i} + \frac{\partial}{\partial y}\vec{j} + \frac{\partial}{\partial z}\vec{k}. \end{cases} \tag{2}$$

Note that besides the definitions of the coordinate axis, velocity components, and the presence of a reference density (ρ_0), the primary difference between Equations 1 and 2 is in the second term of the left-hand side of the equations (i.e. $2\vec{\Omega} \times \vec{v}$ and $f\vec{k} \times \vec{v}$). This term is called the Coriolis Force and represents the effect of the Earth's rotation in the fluid flow. This difference is related to the fact that the rotation effect is function of latitude (θ), so when we assume a Cartesian coordinate system, or represent fluid motions on a tangent plane to the Earth's surface, we are selecting motions that occur around a latitude of reference (θ_0) where the plane is centered.

Since f is the angular rotation frequency of the coordinate axis around z at θ_0, f is constant [$f = f_0 = 2|\vec{\Omega}|sin(\theta_0)$] for a perfect tangent plane, and any effect of the Earth's curvature is filtered out from the solutions of Equation 2. However, some large-scale motions are affected by the this curvature and can not be studied from equations where $f = f_0$ (i.e. f-plane approximation).

So, it is desired to include the curvature effect keeping a coordinate system easy to work with. We can do that by assuming a first order (linear) effect of the Earth's curvature in the rotation meridional change around θ_0 in the sense of a Taylor series expansion. Mathematically f becomes,

$$f = f_0 + \frac{2|\vec{\Omega}|}{a} cos(\theta_0) y = f_0 + \beta y, \tag{3}$$

where a is the Earth's radius. The assumption of the linear relationship between f and the meridional coordinate y is called the β-plane approximation and it has been widely used in GFD studies. A rigorous discussion about its applicability and limitations is found in *Veronis* (1963), *Pedlosky* (1987), and *Verkley* (1990).

Equation 3 shows that at the Equator (θ_0 =0°) f_0 vanishes and therefore $f = \beta y$ ($\beta \approx 2.3\times10^{-11}$ m^{-1} s^{-1}). This representation of the Coriolis parameter received the name of **equatorial β-plane approximation** (*Cushman-Roisin and Beckers*, 1994). Replacing Equation 3 in Equation 2 we get the equations of motion under the equatorial β-plane approximation.

$$\frac{D\vec{v}}{Dt} + \beta y \vec{k} \times \vec{v} = -\frac{\nabla p}{\rho_0} - g'\vec{k} + \nabla \cdot (\frac{\mu}{\rho_0} \nabla \vec{v}). \tag{4}$$

2.1 Length and time scales of motions influenced by rotation

In the previous section, I mentioned that the equatorial large-scale dynamics has some unique characteristics when compared with higher latitudes flows. The most obvious differences are in the length and time scales of these flows, therefore in order to highlight the differences we need to perform a simple scale analysis for different regions of the world's ocean and compare them.

The length scale of flows influenced by rotation are intrinsically linked to the Rossby deformation radius (e.g., *Cushman-Roisin and Beckers*, 1994). This length scale plays an important role in the dynamics of rotating fluids (e.g., Section 2.3) and can be computed by

$$
\begin{aligned}
R_{d0} &= \frac{\sqrt{gH}}{f}; \\
R_{di} &= \frac{\sqrt{g'h}}{f}; \\
g' &= \frac{\rho_2 - \rho_1}{\rho_1} g,
\end{aligned}
\tag{5}
$$

where R_{d0} (R_{di}) is the barotropic (first baroclinic) Rossby deformation radius, H (h) is depth of the water column (pycnocline), and g is the acceleration due to gravity. The quantity g' is called the reduced gravity and corresponds to g scaled by the density difference of the mix-layer (ρ_1) and the pycnocline (ρ_2). If the equatorial β-plane approximation is valid, R_{d0} and R_{di} can be written as

$$
\begin{aligned}
R_{eq0} &= \sqrt{\frac{\sqrt{gH}}{\beta}}; \\
R_{eqi} &= \sqrt{\frac{\sqrt{g'h}}{\beta}}.
\end{aligned}
\tag{6}
$$

Assuming the typical values of $\sqrt{g'h}$ ≈1.4 m s^{-1} and $\sqrt{gH}$ ≈200 m s^{-1} presented by (*Philander*, 1990, Chapter 3) and (*Gill*, 1982, Chapter 11) respectively, the R_{eq0} (R_{eqi}) will be approximately 2000 km (248 km). Note these values are at least twice the Rossby deformation radius for mid and high latitudes ($R_{d0} \leq$ 500 km and $R_{di} \leq$ 50 km). The same reasoning can be applied for the time scale, since the inertial period ($T = \frac{2\pi}{f}$) are of the order of 2 days (≤1 day) at low-latitudes (mid-latitudes) (e.g., *Cushman-Roisin and Beckers*, 1994).

2.2 A note on geostrophy near the Equator

In the tropical region between 10°N and 10°S, the mean upper-ocean (0-500 m depth) circulation in the Atlantic and Pacific is dominated by a complex system of zonal flows (*Talley et al.*, 2011). Basically the major features correspond to the westward flows of the North Equatorial Current (NEC) and South Equatorial Current (SEC), and the eastward flows of the North Equatorial Counter Current (NECC) and

Equatorial Undercurrent (EUC, Figure 1).

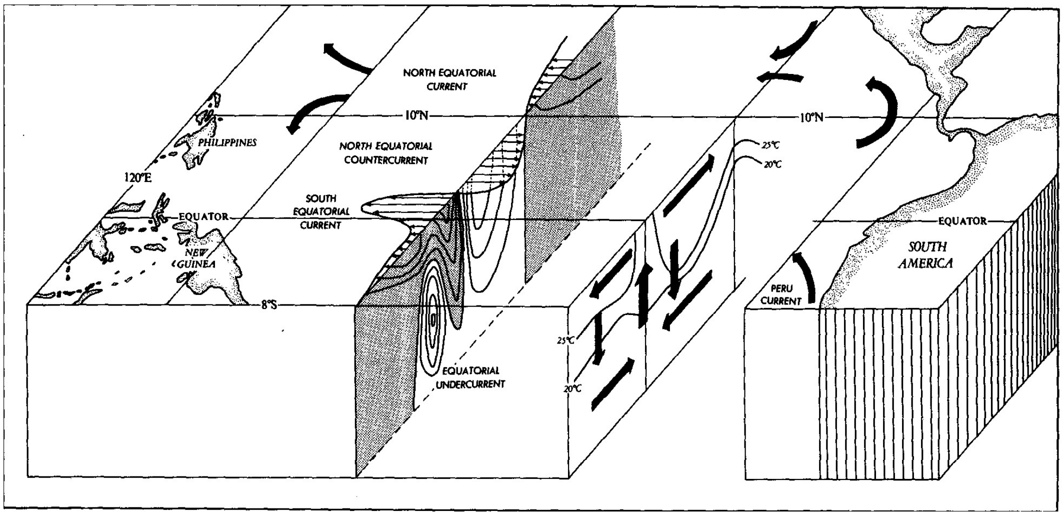

Figure 1: Schematics of the horizontal and vertical circulation of the tropical Pacific Ocean. Source: *Philander et al.* (1987).

Since $\beta y << f_0$ at mid-latitudes, it is intuitive to imagine that the geostrophic balance (i.e. the balance between the Coriolis force and the pressure gradient force) can not be sustained near the Equator, and the steady solution of Equation 4 should be given by a more complex force balance. However theory and observations have shown that this is not the case and the mean SEC and EUC are indeed under geostrophic balance (e.g., *Pedlosky*, 1987; *Lukas and Firing*, 1984).

In contrast to mid-latitudes, the classical zonal geostrophic velocity expression (Equation 7) can not be used to estimate equatorial zonal velocities because it is indeterminate from real data. Additionally, observational noise and small deviations from geostrophy can give rise to spurious meridional pressure gradients, which lead to computational singularities (e.g., *Picaut*, 1989). Hence, several studies based on observations show that the meridionally differentiated form of Equation 7 (Equation 8) can be used to generate good estimates of the velocity structure of the SEC and EUC (*Jerlov*, 1953; *Lukas and Firing*, 1984; *Picaut*, 1989; *Johnson et al.*, 1988; *Joyce et al.*, 1988).

$$fu = -\frac{1}{\rho_0}\frac{\partial p}{\partial y}. \tag{7}$$

$$\beta u_{eq} = -\frac{1}{\rho_0}\frac{\partial^2 p}{\partial y^2}, \tag{8}$$

where u_{eq} is the geostrophic velocity at the Equator.

2.3 Free waves solutions and the equatorial waveguide

The meso and large-scale variability of the equatorial zonal currents are strongly related with the zonal propagation of large eddies and waves (e.g., *Mcphaden and Taft*, 1988; *Philander*, 1990; *Johns et al.*, 1998). In this section, I show that the waves responsible for such variability are solutions of the equations of motion under the equatorial β-plane approximation and what are their main characteristics.

In order to obtain relatively simple solutions and a reasonable representation of the scales of these waves, consider the linear reduced gravity model (1.5-layer model) from (*Philander*, 1990, Chapter 3) represented by the following equations of motion and the continuity equation,

$$\begin{aligned} \frac{\partial u}{\partial t} - \beta y v &= -g' \frac{\partial \eta}{\partial x}, \\ \frac{\partial v}{\partial t} + \beta y u &= -g' \frac{\partial \eta}{\partial y}, \\ g' \frac{\partial \eta}{\partial t} + c^2 \left(\frac{\partial u}{\partial x} + \frac{\partial v}{\partial y}\right) &= 0, \end{aligned} \tag{9}$$

where η is the interface between the upper layer of thickness H (or the pycnocline depth) and the motionless lower layer, $c^2 = g'H$, and the Equator is centered at $y = 0$.

2.3.1 The wave guide

Assuming a stationary solution of Equation 9 described by the stream function $\Psi(x,y)$ ($u = 0 = -\frac{\partial \Psi}{\partial y}$ and $v = 0 = \frac{\partial \Psi}{\partial x}$) and a lower order perturbation $\Psi'(x,y,t)$, it is possible to write the vorticity equation for this model as

$$\frac{\partial}{\partial t}[\nabla_H^2 \Psi' - (\frac{\beta y}{c})^2 \Psi'] + \beta \frac{\partial \Psi'}{\partial x} = 0 \tag{10}$$

, where the ∇_H^2 is the horizontal Laplacian operator. Since Equation 9 is valid only in tropical regions, it is reasonable imagine wave-like perturbations of the form $\Psi' = \hat{\Psi}(y) exp[i(kx - \omega t)]$ which leads Equation 10 to become

$$\frac{\partial^2\hat{\Psi}}{\partial y^2} + \frac{1}{R_{eqi}^4}(Y^2 - y^2)\hat{\Psi} = 0,$$
$$Y^2 = [(\frac{\omega}{c})^2 - k^2 - \frac{\beta k}{\omega}]R_{eqi}^4. \tag{11}$$

The physically meaningful solutions of Equation are oscillatory and decay exponentially towards latitudes $\pm Y$, which consists of an equatorial/tropical zone of width $2Y$. Therefore the equatorial belt acts as a waveguide, and the waves tend to trapped (e.g., *Philander*, 1990). Note that the dimension of Y is scaled by the equatorial Rossby deformation radius, which will determine the decaying rate of the solution.

2.3.2 Equatorial Kelvin waves

One of the most important trapped waves solution of Equation 9 is the equatorial Kelvin wave. In this case, the equator (y =0) works as a solid boundary where no meridional flow is allowed. As the coastal Kelvin wave, it propagates with phase velocity c however the solution for u, v and η are

$$\eta = e^{-\frac{y^2}{2R_{eqi}^2}} e^{i(kx-\omega t)},$$
$$u = (\frac{g'}{c}) e^{-\frac{y^2}{2R_{eqi}^2}} e^{i(kx-\omega t)}, \tag{12}$$
$$v = 0.$$

As shown in Equation 12, the amplitude of the Kelvin waves will decay poleward if c >0 ($R_{eqi}^2 = \frac{c}{\beta}$). Therefore equatorial Kelvin waves are non-dispersive waves, that propagate phase eastward and its amplitude decays polewards.

2.3.3 Equatorial Rossby and Inertia-Gravity waves

Back to the vorticity Equation 10, lets suppose that the perturbation has a meridional propagation and the y dependence of the oscillatory part is given by $exp[i(kx + ly + \omega t)]$. Since the waves can not propagate to regions where $|y| > Y$, the superpositions of the continuously reflected waves of same k and ω will generate standing latitudinal modes, or equatorially trapped modes (see *Philander*, 1990, for more details).

In this case, the dispersion relation obtained is given by

$$\frac{c}{\beta}[(\frac{\omega}{c})^2 - k^2 - \frac{\beta k}{\omega}] = 2n+1, \tag{13}$$

where n is the latitudinal mode ($n = 1, 2, 3 ...$). On the lower frequencies limit, the $\frac{\omega}{c})^2$ term from Equation 13 is small when compared to the other terms and the dispersion relation can be written as

$$\omega \approx \frac{-\beta k}{k^2 + \frac{2n+1}{R_{eqi}^2}}. \tag{14}$$

Equation 14 corresponds to the dispersion relation of equatorially trapped Rossby waves. These dispersive waves propagate phase westward and corresponds to an important phenomena in the equatorial dynamics. In fact, *Philander et al.* (1984) the numerical experiments show that the combination of eastward-propagating equatorial Kelvin waves and westward-propagating Rossby waves explains the general behavior of the thermocline displacements during a El Niño Southern Oscillation (ENSO) event on the Pacific (Figure 2).

On the high frequencies limit, where $\frac{\beta k}{\omega}$ is small, and $n \geq 1$ the dispersion relation becomes

$$\omega^2 \approx (2n+1)\beta c + k^2 c^2. \tag{15}$$

The solution described by Equation 15 corresponds to the Inertia-Gravity waves at the equatorial region, also known as trapped equatorially trapped Poincare waves.

Interestingly, with no approximation is made and the dispersion relations of $n = 0$ is studied, a exclusive equatorial wave class comes out from Equation 13, the so called mixed planetary-gravity waves or Yanai waves (*Gill*, 1982). Yanai waves are unique in that for large positive k it behaves as a gravity wave, whereas for large negative k it behaves as a Rossby wave. *Johns et al.* (1998) attribute the monthly fluctuations of the EUC meridional velocity measurements with the propagations of Yanai waves. Figure 3 presents the dispersion relations curves of the free waves discussed in this documents.

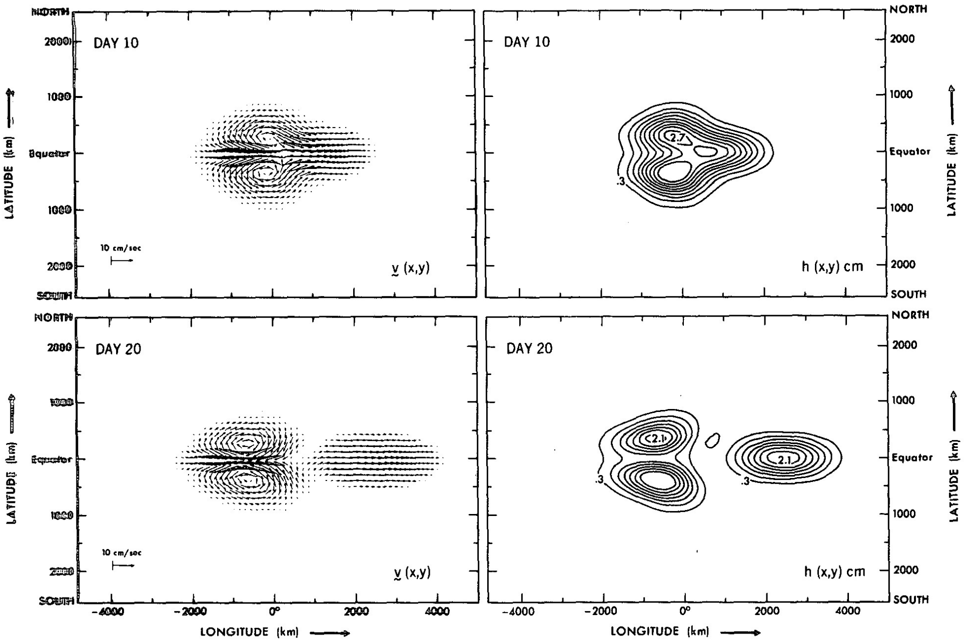

Figure 2: The dispersion of an initially bell-shaped thermocline displacement into an eastward-propagating Kelvin wave and westward-propagating Rossby waves during a simulated ENSO event. Left panels show the horizontal currents and the right panels the termocline displacements. Source: *Philander et al.* (1984).

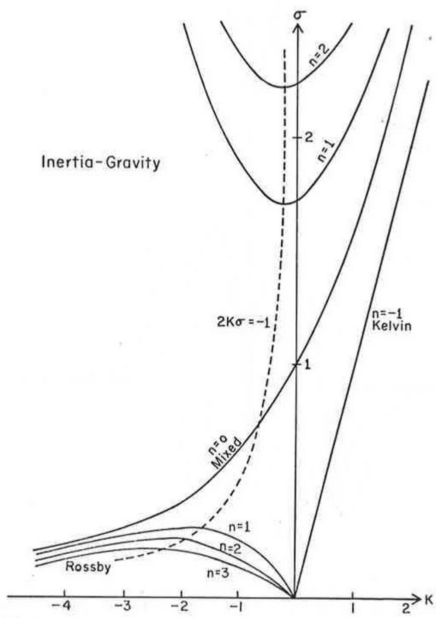

Figure 3: Dispersion diagram for equatorially trapped waves. The unit of frequency (σ) is $[(\beta c)^{1/2}]$ and the unit of k is the inverse of R_{eqi}. Source: *Cane and Sarachik* (1976).

References

Cane, M. A., and E. S. Sarachik (1976), Forced baroclinic ocean motions I. The linear equatorial unbounded case., *J. Mar. Res.*, *34*(4), 629–665.

Cushman-Roisin, B., and J.-M. Beckers (1994), *Introduction to Geophysical Fluid Dynamics: Physical and Numerical Aspects*, 2ªed., Elsevier.

Gill, A. E. (1982), *Atmosphere-ocean dynamics*, vol. 30, Academic press.

Jerlov, N. G. (1953), Studies of the equatorial currents in the Pacific, *Tellus*, *5*, 308–314.

Johns, W. E., T. N. Lee, R. C. Beardsley, J. Candela, R. Limeburner, and B. Castro (1998), Annual Cycle and Variability of the North Brazil Current, *J. Phys. Oceanogr.*, *28*, 103–128.

Johnson, E. S., L. A. Regier, and R. A. Knox (1988), A study of geostrophy in tropical Pacific Ocean currents during the NORPAX Tahiti Shuttle using a shipboard Doppler acoustic current profiler, *J. Phys. Oceanogr.*, *18*, 708–723.

Joyce, T. M., R. Lukas, and E. Firing (1988), On the hydrostatic balance and equatorial geostrophy, *Deep-Sea Res.*, *35*(8), 1255–1257.

Lukas, R., and E. Firing (1984), The geostrophic balance of the Pacific equatorial undercurrent, *Deep-Sea Res.*, *31*, 61–66.

Mcphaden, M. J., and B. A. Taft (1988), Dynamics of Seasonal and Intraseasonal Variability in the Eastern Pacific, *J. Phys. Oceanogr.*, *18*, 1703–1732.

Pedlosky, J. (1987), *Geophysical Fluid Dynamics*, second ed., Springer.

Philander, S. G. (1990), *El Niño, La Niña, and the southern oscillation*, Academic press.

Philander, S. G. H., T. Yamagata, and R. C. Pacanowski (1984), Unstable Air-Sea Interactions in the Tropics, *J. Atmos. Sci.*, *41*(4), 604–613.

Philander, S. G. H., W. J. Hurlin, and A. D. Seigel (1987), Simulation of seasonal cycle of the tropical Pacific ocean, *J. Phys. Oceanogr.*, *17*, 1986–2002.

Picaut, J. (1989), Use of the Geostrophic Approximation to Estimate Time-Varying Zonal Currents at the Equator, *J. Geophys. Res.*, *94*(C3), 3228–3236.

Talley, L. D., G. L. Pickard, W. J. Emery, and J. H. Swift (2011), *Descriptive Physical Oceanography: An Introduction*, sixth ed., Academic Press.

Verkley, W. T. M. (1990), On the beta-plane approximation. Journal of the Atmospheric Sciences, *J. Atmos. Sci.*, *47*, 2453–2460.

Veronis, G. (1963), On the approximations involved in transforming the equations of motion from a spherical surface to the β-plane. I. Barotropic systems, *J. Mar. Res.*, *21*, 110–124.